

Plasma-treated carbonyl iron particles as a dispersed phase in magnetorheological fluids

Michal Sedlacik^{a,b}, Vladimir Pavlinek^{a,b}, Marian Lehocky^a, Ales Mracek^{a,c}, Ondrej Grulich^c,
Petra Svrcinova^d, Petr Filip^d and Alenka Vesel^e*

^a Centre of Polymer Systems, University Institute, Tomas Bata University in Zlin, Nad Ovcirnou 3685,
760 01 Zlin, Czech Republic

^b Polymer Centre, Faculty of Technology, Tomas Bata University in Zlin, namesti T. G.
Masaryka 275, 762 72 Zlin, Czech Republic

^c Department of Physics and Materials Engineering, Faculty of Technology, Tomas Bata University in
Zlin, namesti T. G. Masaryka 275, 762 72 Zlin, Czech Republic

^d Institute of Hydrodynamics, Academy of Sciences of the Czech Republic, Pod Patankou 30/5, 160 00
Prague 6, Czech Republic

^e Department for Surface Engineering and Optoelectronics, Jozef Stefan Institute, Jamova cesta 39,
1000 Ljubljana, Slovenia

* pavlinek@ft.utb.cz (email of corresponding author), tel: +420 576 031 205, fax: +420 576 031 444

ABSTRACT

The aim of this paper is to document suitability of plasma-treated carbonyl iron particles as a dispersed phase in magnetorheological fluids. Surface-modified carbonyl iron particles were prepared via their exposure to 50% argon and 50% octafluorocyclobutane plasma. The X-ray photoelectron spectroscopy was used for analysis of chemical bonding states in the surface layer. Plasma-treated particles were adopted for a dispersed phase in magnetorheological (MR) fluids, and the MR behaviour was investigated using rotational rheometer equipped with magnetic field generator. Viscoelasticity changes of MR fluids were measured in the small-strain oscillatory shear flow as a function of the strain amplitude, frequency and the magnetic flux density. The MR fluids based on plasma-treated particles exhibit promoted suspension stability, which is attributed to the interactions between fluorine bonded on particle surface and methyl groups of silicone oil.

KEYWORDS: Carbonyl iron; Magnetorheological fluid; Plasma; Viscoelasticity

1. Introduction

The possibility to control the flow and deformation of magnetorheological (MR) fluids by application of a magnetic field classified these systems into smart and intelligent materials. MR fluids are suspensions of non-colloidal ($\sim 1\text{--}10\ \mu\text{m}$), multi-domain ferromagnetic, ferrimagnetic particles dispersed in a non-magnetic carrier fluid [1–3]. The suspensions exhibit nearly Newtonian behaviour with values of apparent viscosity ranging from 0.1 to 1 Pa s at low shear rates in the absence of external magnetic field. However, when the field is applied, the particles become **magnetized** and the chain-like structures are formed within the fluid due to the dipolar magnetic interactions. The formation of internal structure leads to an abrupt transformation within milliseconds from liquid to solid-like state, which is caused by drastic changes of rheological properties of the suspension such as an enhancement of apparent viscosity, yield stress or viscoelastic moduli [4–6]. The particles can return to an unorganized state, and the apparent viscosity is reduced to the original value, when the magnetic field is removed. Analogous variant to MR fluids are electrorheological fluids, in which the chain-like structure is created under external electric field [7]. The ability of MR fluids to change the apparent viscosity depending on the intensity of external magnetic field can be used in torque transducers [8,9], active controllable dampers [10,11] as well as in cancer therapy [12,13], etc.

However, the poor stability of MR fluids due to sedimentation still hinders their larger utilization by reason that non-uniform particle distribution can interfere with MR response. The excessive gravitational settling is caused by the density mismatch between magnetic particles (e.g., bare carbonyl iron = $7.86\ \text{g}\cdot\text{cm}^{-3}$) and carrier liquid (e.g., silicone oil = $0.97\ \text{g}\cdot\text{cm}^{-3}$). To overcome this crucial problem, different methods such as the use of viscoplastic media [14], adding **special type of additives (carbon nanotube)** [15], **core-shell structured particles** [16,17], the use of aqueous suspensions stabilized by acrylic acid polymers [18], adding surfactants (oleic acid) [19], the use of

bidisperse MR fluids [20] or choice of water-in-oil emulsion as a continuous phase [21] have been proposed. Nevertheless, further improvement of the stability of MR fluids is necessary.

Recently, there is growing interest in using low-temperature plasma to modify the surface of variety of materials [22,23]. It is a powerful technique, since the surface properties of materials can be changed without affecting of their bulk properties [24]. The Teflon-like surface thin film is prepared in plasma discharge using octafluorocyclobutane (C₄F₈) as a carrier gas with an admixture of argon [25,26].

In the present study, plasma-treated particles of carbonyl iron (CI) were obtained after exposition of bare magnetic particles in 50% argon + 50% octafluorocyclobutane processing gas for different times of exposure. Effects of the surface modification on viscosity, viscoelastic properties of MR fluid containing plasma-treated particles and long-term stability were evaluated.

2. Materials and methods

2.1 Materials

Carbonyl iron particles (HQ and SL grades, BASF, Germany) were selected as magnetic agents. The main material characteristics of HQ and SL grades of bare CI are following: spherical shape of particles with the average size of about 1 μm and 9 μm, non-modified surface, and content of α-iron > 97 % and > 99.5 %, respectively. As components of processing gas, argon (Ar purity ≥ 99.998, Messer Industriegase GmbH, Germany) and octafluorocyclobutane (C₄F₈ purity ≥ 99.998, Linde AG, Germany) were used.

2.2 Plasma treatment of particles

The surface modification of CI particles was performed using a plasma reactor Diener Femto (Diener Electronic, USA) operating at frequency 40 kHz. The samples were inserted into the rotating rectangular parallelepiped glass reaction chamber which was placed inside of the plasma reactor. Such configuration enables the uniform modification of powdered samples. CI powders were exposed to 50% Ar and 50% C₄F₈ plasmas sustained at power of 50 W at processing gas pressures of approx. 30 – 40 Pa with the processing gas flow rate of 90 sccm. After certain time, the plasma was quenched and samples were kept under the atmosphere of processing gas for next 5 minutes. Three types of samples (B, C, D) were obtained in this way varying in the time of modification and CI grade (Tab. 1).

Table 1. Parameters of samples and their surface composition from XPS.

Sample	Particle size	Treatment time	C 1s	O 1s	N 1s	F 1s	Fe 2s
	[μm]	[s]	[%]	[%]	[%]	[%]	[%]

A	1	0	22.2	50.1	0	0	27.7
B	1	120	15.5	45.0	2.2	6.5	30.8
C	1	300	27.9	40.7	1.6	6.4	23.4
D	9	120	25.9	41.3	0	7.4	25.4

2.3 Characterization of particles surface composition

Surface characteristics of non-treated and plasma treated CI particles were observed with XPS (X-ray photoelectron spectroscopy, TFA XPS, Physical Electronics, USA). The base pressure in the chamber was about 6×10^{-8} Pa. The samples were excited with X-rays over a 400- μm spot area with a monochromatic Al $K_{\alpha 1,2}$ radiation at 1486.6 eV. Photoelectrons were detected with a hemispherical analyzer positioned at the angle of 45° with respect to the sample surface. Survey-scan spectra were made at pass energy of 187.85 eV and an energy step was 0.4 eV. The concentrations of elements were determined by using MultiPak v7.3.1 software from Physical Electronics, which was supplied with the spectrometer [27].

2.4 Characterization of magnetorheological fluids

MR fluids containing 80 wt.% of bare CI (HQ or SL grade) or their plasma-treated analogues in silicone oil (Lukosiol M200, Chemical Works Kolín, Czech Republic; viscosity of 200 mPa s, density of 0.965 g cm^{-3}) were prepared. Suspensions were mechanically stirred before each measurement. MR characteristics of the suspensions in steady and oscillatory shear were examined using a rotational rheometer Physica MCR501 (Anton Paar GmbH, Austria) with the Physica MRD 180/1T magneto-cell at 25°C . True magnetic flux density was measured using a Hall probe and temperature was checked with the help of an inserted thermocouple, for details see [28]. Temperature was set using an Anton Paar circulator Viscotherm VT2 with temperature stability $\pm 0.02^\circ\text{C}$. Maximum magnetic flux density used in all measurements did not exceed 0.3 T to ensure sufficient homogeneity of a magnetic field perpendicular to the shear flow direction. A parallel-plate measuring system with diameter of 20 mm and gap of 1 mm was used.

2.5 Stability test

Stability of the various types of CI particles based MR suspensions was examined by a sedimentation ratio test which is a simple naked-eye observation of sedimentation. In this method, a set of the samples were placed in test tubes and observed for 24 hrs. The settling of the macroscopic phase boundary between the concentration suspension and the relatively clear oil-rich phase was measured as a function of time. Then, the sedimentation ratio is defined as the height of particle-rich phase relative to the total suspension height.

3. Results and discussion

3.1 Surface composition

Chemical bonding states of the nano-surface layer of CI powders exposed to plasma were observed via X-ray photoelectron spectroscopy. Figure 1 shows XPS spectra for bare and plasma-treated CI samples composed of four main components: C 1s peak at binding energy of 284.6 eV, O 1s peak at 531.6 eV, F 1s peak at 684.9 eV, and Fe 2s peak at 706.8 eV [27]. Here it should be noted that the other peaks are from signals of non-valent Auger electrons.

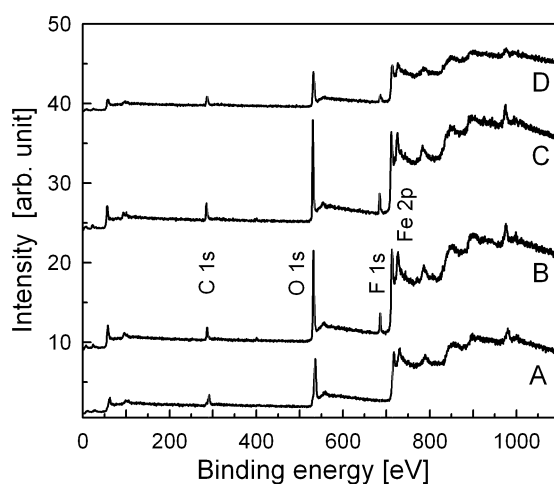


Fig. 1. XPS spectra for CI samples without and with exposure to Ar + C₄F₈ plasma.

The results listed in Tab. 1 show that the amount of O 1s, which was presented on the CI surface may be due to oxidation of carbon and iron in the air, decreased due to Ar + C₄F₈ plasma. Furthermore, based on these data it was also suggested that the reduced O 1s was efficiently substituted by bonded F 1s. A certain amount of N 1s present in the particles surface layer after plasma treatment can be attributed to the post-plasmatic reaction ongoing in the air. Figure 2 shows the atomic ratios of F/Fe on the surface of CI without and with exposure to Ar + C₄F₈ plasma. As can be seen, the ratio increases both with treatment time and with the particle size. The larger amount of bonded fluorine on larger particles can result from a fact that smaller particles had strong interface attractive forces and formed agglomerates which implicated smaller surface area than larger ones. Above mentioned features indicate that the plasma treatment of CI particles can change their surface properties having a positive effect on their practical use.

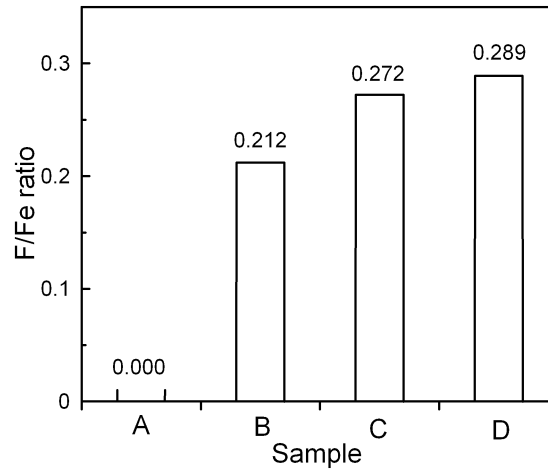


Fig. 2. Atomic ratio of F/Fe for CI samples without and with exposure to Ar + C₄F₈ plasma.

3.2 Steady shear and yield stress

Rheological behaviour of MR suspensions based on non-treated and plasma-treated CI particles was investigated in a controlled shear-rate mode in static magnetic field ranging from 0 to 0.3 T. The measurements under given conditions were repeated twice and an average value was used for further evaluation. During each run under a magnetic field, the MR suspension was first sheared ($\dot{\gamma} = 100 \text{ s}^{-1}$) at zero magnetic field for 60 s to distribute the particles uniformly and after the measurement the system was completely demagnetized to disturb residual internal structures. Figure 3 displays shear stress as a function of shear rate for samples A and B based MR fluids under different external magnetic flux densities.

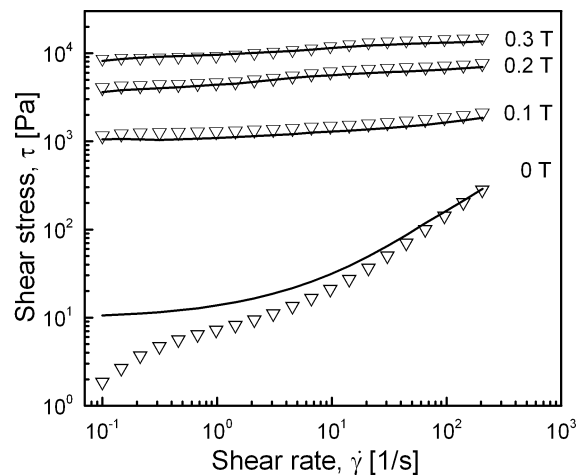


Fig. 3. Rheogram of 80 wt.% MR fluids based on samples A (open triangles) and B (lines) under various magnetic fields applied.

In the absence of magnetic field, the MR suspension containing non-treated particles exhibits nearly Newtonian behaviour, while suspensions with plasma-treated particles provide a certain value of yield

stress, which can be generated due to interaction forces between fluorine bonded on CI particles and methyl groups of silicone oil. In the presence of magnetic field, both systems exhibit Bingham plastic behaviour showing that the magnetic particles were aligned into the chain-like structure sufficiently rigid to withstand certain deforming stresses without any external manifestation of flow. Typically for MR fluids, the shear stress of samples A and B based MR fluids increased for the entire shear rate region with the increase of magnetic flux density [29]. When magnetic field is applied, the magnetic forces between polarized particles strongly dominate over the interaction ones between plasma-treated particles and silicone oil, thus both MR suspensions have approximately the same values of shear stress irrespective of employed particles.

From the courses of shear stress–shear rate curves, dynamic yield stresses can be obtained by fitting the experimental data with the Cho–Choi–Jhon model [30]:

$$\tau = \frac{\tau_0}{1 + (t_2 \dot{\gamma})^\alpha} + \eta_\infty \left(1 + \frac{1}{(t_3 \dot{\gamma})^\beta} \right) \dot{\gamma} \quad (1)$$

Here, τ_0 is the dynamic yield stress, α is related to the decrease in the stress, t_2 and t_3 represent time constants, β is the exponent in the range $0 < \beta \leq 1$, and η_∞ is the viscosity at high shear rates and is interpreted as the viscosity in the absence of a magnetic field [30].

Table 2 shows the yield stresses and optimal parameters for the Cho–Choi–Jhon model for MR suspensions based on CI particles (samples A–D) at the magnetic flux density of 0.3 T. Evidently from Table 2, suspension with CI particles of sample B exhibits almost the same value of τ_0 as non-treated particles (sample A) based MR suspension in the magnetic field of 0.3 T. Further, increase in time of plasma treatment (sample C) led to lower τ_0 and this can be explained by the lower iron content in the surface layer at the expense of higher carbon content. Thus, 120 s exposure appears as an optimal treatment time of CI particles from the magnetorheological point of view. It was also found from the results in Table 2, that larger CI particles (i.e. sample D) based MR suspension possesses almost twice higher value of τ_0 due to larger magnetic domains.

Table 2. Parameters of the Cho–Choi–Jhon model obtained by linear regression for various treated CI particles–based MR fluids at the magnetic flux density of 0.3 T.

Parameters	A	B	C	D
τ_0 [Pa]	8 863	8 796	7 485	16 182
t_2 [s]	0.0011	0.0011	0.2150	0.7013
α [–]	0.0006	0.0006	0.1191	0.5641
η_∞ [Pa s]	1.1992	1.1992	1.1967	1.1992

t_3 [s]	7.8×10^{-5}	7.8×10^{-5}	7.4×10^{-5}	2.2×10^{-5}
β [-]	0.8820	0.8850	0.8433	0.7991

3.3 Viscoelastic properties

Oscillatory shear tests represent an effective way to study the dynamic characteristics of microstructures formed in MR suspensions. Figure 4 presents the storage modulus, G' , (elastic behaviour) and loss modulus, G'' , (viscous behaviour) versus strain for sample B suspension under various magnetic flux densities. Both G' and G'' increase rapidly from their original values upon the application of a magnetic field over the whole strain range ($\gamma = 10^{-5} - 10^{-2}$ in our case). Moreover, G' comes to be significantly higher than G'' in the linear viscoelastic region (LVR), i.e. in the range of independency of G' and G'' on strain amplitude, and the difference between these moduli grows also with magnetic flux density. This dramatic change in rheological properties originates from the magnetic dipole-dipole interactions between CI particles resulting in the formation of chain-like structures.

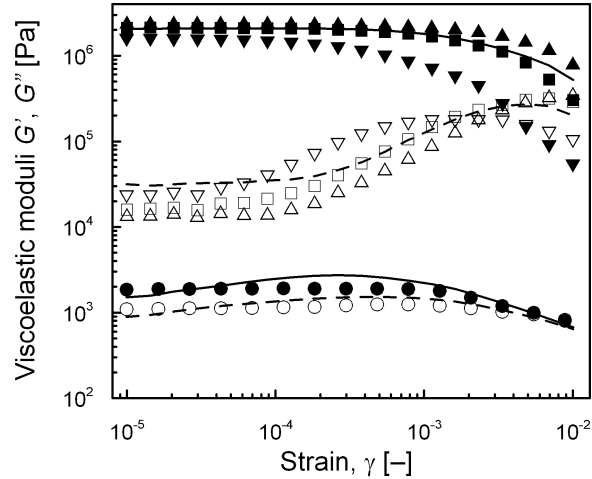


Fig. 4. Storage, G' , (solid symbols or line) and loss, G'' , (open symbols or dashed line) moduli versus strain, γ , at angular frequency of 62.83 rad s^{-1} for 80 wt.% MR fluid based on samples A (lines) particles under magnetic flux density (T) of 0 or 0.3, and B (symbols) particles under various magnetic fields applied. The symbols for magnetic flux densities (T): (\bullet, \circ) 0; ($\blacktriangledown, \triangledown$) 0.1; (\blacksquare, \square) 0.2; ($\blacktriangle, \triangle$) 0.3.

Figure 5 shows viscoelastic moduli G' and G'' as functions of angular frequency at a small strain of 2×10^{-4} in the LVR for 80 wt.% MR suspension based on CI particles of sample B under various magnetic fields. In the absence of magnetic field, G' is slightly larger than G'' , which can be due to high CI particle loading in the suspension. Upon application of the external magnetic field G' and G''

increase in three and two orders of magnitude, respectively. As can be seen in Fig. 5, G' values are either constant or increase slightly as the angular frequency rises up to 100 rad s^{-1} . This is typical behaviour of stiff three-dimensional network formed by magnetized CI particles within MR fluid which is sufficiently strong to transmit the elastic force in such system [31].

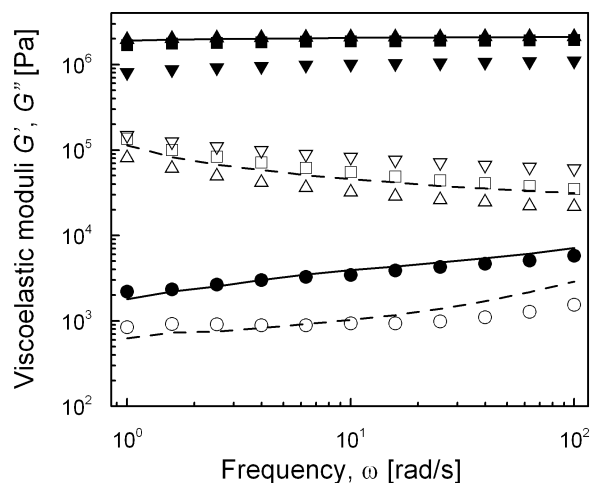


Fig. 5. Storage, G' , (solid symbols or line) and loss, G'' , (open symbols or dashed line) moduli versus angular frequency, ω , for samples A (lines) particles under magnetic flux density (T) of 0 or 0.3, and B particles based MR suspension (80 wt.%) under various magnetic fields applied. The symbols for magnetic flux densities (T): (●,○) 0; (▼,▽) 0.1; (■,□) 0.2; (▲,△) 0.3.

3.4 Sedimentation test

Finally, the effect of CI plasma treatment on the sedimentation stability was investigated. The MR fluids with overall fraction of 50 wt.% of HQ grade CI particles were set in static conditions and sedimentation ratios were measured for 24 hrs. Figure 6 shows the effect of the exposure of CI particles to Ar + C₄F₈ plasma on the sedimentation stability of MR suspensions based on these particles. Three kinds of CI particles were used for the examination varying in treatment time (i.e. samples A, B, and C). The inset photo shows final results of the sedimentation after 24 hrs for all suspensions. The interactions between fluorine bonded on the CI surface and methyl groups of silicone oil seem to be present, resulting in the retardation of sedimentation. Moreover, the MR suspension based on CI particles with 120 s exposure to plasma exerted the best suspension stability even better than in case of 300 s treated ones. This is probably caused by the growth of surface layer and so the overall particle size with increasing treatment time, which was confirmed using dynamic light scattering technique (Zetasizer, Malvern Instruments, UK). The particles size for 0, 120, and 300 s exposure to plasma time matched to 1, 1.026, and 1.038 μm , respectively. Therefore, there is an optimum plasma treatment time of 120 s for 1 μm CI particles ensuring the best combination of MR

performance and suspension stability. However, 300 s plasma treated particles suspension possess still higher stability due to the fluorine–methyl group interactions than for non–treated CI particles suspension. In other words it can be said that the retardation of sedimentation can be enhanced by surface modification of magnetic particles in plasma in order to improve the interactions between particles and carrier liquid without the use of further viscosity modifying components [32].

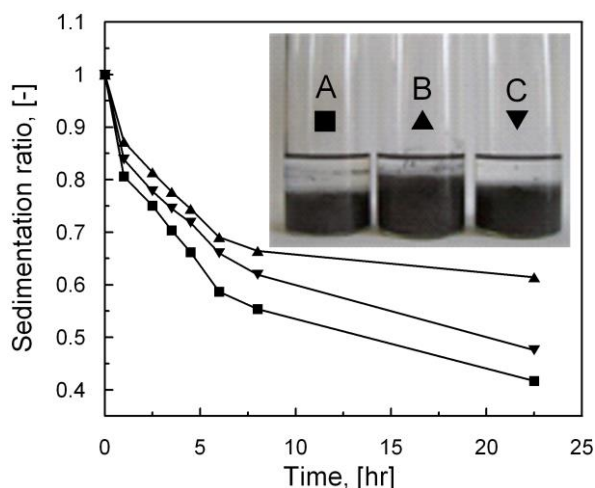


Fig. 6. Sedimentation ratio versus time for sample A (■), B (▲), C (▼) based MR suspensions (50 wt.%) in 200 mPa s silicone oil.

4. Conclusions

Magnetic CI particles with different size were exposed to 50% argon and 50% octafluorocyclobutane plasma for different times for bonding of fluorine on their surface and its presence was confirmed via X–ray photoelectron spectroscopy. The plasma–treated particles based MR fluids show typical MR characteristics including high values of yield stresses and the sharp shear thinning behaviour under external magnetic field applied. The viscoelastic properties of the fluids suggest that plasma–treated CI particles MR suspensions exhibit strong elastic behaviour within the linear viscoelastic region due to the robust chain structure under a magnetic field applied. Compared with MR fluid based on bare CI, plasma–treated CI particles based MR fluids show enhanced sedimentation stability, and it seems to be due to the interaction forces between fluorine bonded on particle surface and methyl groups of silicone oil.

Acknowledgements

The authors wish to thank to the Ministry of Education, Youth and Sports of the Czech Republic (MSM7088352101) and the Czech Science Foundation (project 104/09/H080) for financial support.

This article was written with support of Operational Program Research and Development for Innovations co-funded by the European Regional Development Fund (ERDF) and national

budget of Czech Republic, within the framework of project Centre of Polymer Systems (reg. number: CZ.1.05/2.1.00/03.0111).

References

- [1] G. Bossis, O. Volkova, S. Lacis, A. Meunier, *Magnetorheology: Fluids, Structures and Rheology*, Lect. Notes Phys. 594 (2002) 202–230.
- [2] I. Bica, H.J. Choi, Preparation and electro-thermoconductive characteristics of magnetorheological suspensions, *Int. J. Mod. Phys. B* 22 (2008) 5041–5064.
- [3] I. Bica, Advances in magnetorheological suspension: Production and properties, *J. Ind. Eng. Chem.* 12 (2006) 501–515.
- [4] **J. de Vicente, D.J. Klingenberg, R. Hidalgo-Alvarez, Magnetorheological fluids: a review, *Soft Matter* 7 (2011) 3701–3710.**
- [5] **B.J. Park, F.F. Fang, H.J. Choi, Magnetorheology: materials and application, *Soft Matter* 6 (2010) 5246–5253.**
- [6] L.K. Yang, F. Duan, A. Eriksson, Analysis of the optimal design strategy of a magnetorheological smart structure, *Smart Mater. Struct.* 17 (2008) 015047.
- [7] M. Stenicka, V. Pavlinek, P. Saha, N.V. Blinova, J. Stejskal, O. Quadrat, Effect of hydrophilicity of polyaniline particles on their electrorheology: Steady flow and dynamic behaviour, *J. Colloid Interface Sci.* 346 (2010) 236–240.
- [8] V.A. Neelakantan, G.N. Washington, Modeling and reduction of centrifuging in magnetorheological (MR) transmission clutches for automotive applications, *J. Intel. Mat. Syst. Str.* 16 (2005) 703–711.
- [9] K.H. Gudmundsson, F. Jonsdottir, F. Thorsteinsson, A geometrical optimization of a magnetorheological rotary brake in a prosthetic knee, *Smart Mater. Struct.* 19 (2010) 035023.
- [10] S.N. Madhekar, R.S. Jangid, Variable dampers for earthquake protection of benchmark highway bridges, *Smart Mater. Struct.* 18 (2009) 115011.
- [11] J.H. Koo, F.D. Goncalves, M. Ahmadian, A comprehensive analysis of the response time of MR dampers, *Smart Mater. Struct.* 15 (2006) 351–358.
- [12] L.E. Udrea, N.J.C. Strachan, V. Badescu, O. Rotariu, An in vitro study of magnetic particle targeting in small blood vessels, *Phys. Med. Biol.* 51 (2006) 4869–4881.

- [13] M.O. Aviles, A.D. Ebner, J.A. Ritter, Ferromagnetic seeding for the magnetic targeting of drugs and radiation in capillary beds, *J. Magn. Magn. Mater.* 310 (2007) 131–144.
- [14] P.J. Rankin, A.T. Horvath, D.J. Klingenberg, Magnetorheology in viscoplastic media, *Rheol. Acta* 38 (1999) 471–477.
- [15] **F.F. Fang, H.J. Choi, M.S. Jhon, Magnetorheology of soft magnetic carbonyl iron suspension with single-walled carbon nanotube additive and its yield stress scaling function, *Colloid Surf. A-Physicochem. Eng. Asp.* 351 (2009) 46–51.**
- [16] **M. Sedlacik, V. Pavlinek, P. Saha, P. Svrčinová, P. Filip, J. Stejskal, Rheological properties of magnetorheological suspensions based on core-shell structured polyaniline-coated carbonyl iron particles, *Smart Mater. Struct.* 19 (2010) 115008.**
- [17] **F.F. Fang, H.J. Choi, Y. Seo, Sequential Coating of Magnetic Carbonyliron Particles with Polystyrene and Multiwalled Carbon Nanotubes and Its Effect on Their Magnetorheology, *ACS Appl. Mater. Interfaces* 2 (2010) 54–60.**
- [18] J.L. Viota, A.V. Delgado, J.L. Arias, J.D.G. Duran, Study of the magnetorheological response of aqueous magnetite suspensions stabilized by acrylic acid polymers, *J. Colloid Interface Sci.* 324 (2008) 199–204.
- [19] M. Lopez–Lopez, J. de Vicente, F. Gonzales–Caballero, J.D.G. Duran, Stability of magnetizable colloidal suspensions by addition of oleic acid and silica nanoparticles, *Colloid Surface A* 264 (2005) 75–81.
- [20] N.M. Wereley, A. Chaudhuri, J.H. Yoo, S. John, S. Kotha, A. Suggs, R. Radhakrishnan, B.J. Love, T.S. Sudarshan, Bidisperse magnetorheological fluids using Fe particles at nanometer and micron scale, *J. Intel. Mat. Syst. Str.* 17 (2006) 393–401.
- [21] J.H. Park, B.D. Chin, O.O. Park, Rheological properties and stabilization of magnetorheological fluids in a water-in-oil emulsion, *J. Colloid Interface Sci.* 240 (2001) 349–354.
- [22] M. Lehocky, H. Drnovska, B. Lapcikova, A.M. Barros-Timmons, T. Trindade, M. Zembala, L. Lapcik, Plasma surface modification of polyethylene, *Colloid Surf. A-Physicochem. Eng. Asp.* 222 (2003) 125–131.

- [23] Z. Adamczyk, L. Szyk-Warszynska, M. Zembala, M. Lehocky, In situ studies of particle deposition on non-transparent substrates, *Colloid Surf. A-Physicochem. Eng. Asp.* 235 (2004) 65–72.
- [24] M. Sowe, I. Novak, A. Vesel, I. Junkar, M. Lehocky, P. Saha, I. Chodak, Analysis and Characterization of Printed Plasma-Treated Polyvinyl Chloride, *Int. J. Polym. Anal. Charact.* 14 (2009) 641–651.
- [25] M. Lehocky, P. Stahel, M. Koutny, J. Cech, J. Institoris, A. Mracek, Adhesion of *Rhodococcus* sp S3E2 and *Rhodococcus* sp S3E3 to plasma prepared Teflon-like and organosilicon surfaces, *J. Mater. Process. Technol.* 209 (2009) 2871–2875.
- [26] M. Lehocky, P.F.F. Amaral, P. Stahel, M.A.Z. Coelho, A.M. Barros-Timmons, J.A.P. Coutinho, Deposition of *Yarrowia lipolytica* on plasma prepared teflonlike thin films, *Surf. Eng.* 24 (2008) 23–27.
- [27] J.F. Moulder, W.F. Stickle, P.E. Sobol, K.D. Bomben, *Handbook of X-Ray Photoelectron Spectroscopy*, Eden Prairie, Minnesota, 1995.
- [28] H.M. Laun, C. Gabriel, Measurement modes of the response time of a magneto-rheological fluid (MRF) for changing magnetic flux density, *Rheol. Acta* 46 (2007) 665–676.
- [29] B.J. Park, S.M. Kim, H.J. Choi, Fabrication and magnetorheological property of core/shell structured magnetic composite particle encapsulated with cross-linked poly(methyl methacrylate), *Mater. Lett.* 63 (2009) 2178–2180.
- [30] M.S. Cho, H.J. Choi, M.S. Jhon, Shear stress analysis of a semiconducting polymer based electrorheological fluid system, *Polymer* 46 (2005) 11484–11488.
- [31] K. Tsuda, Y. Takeda, H. Ogura, Y. Otsubo, Electrorheological behavior of whisker suspensions under oscillatory shear, *Colloid Surf. A-Physicochem. Eng. Asp.* 299 (2007) 262–267.
- [32] J. de Vicente, M. Lopez–Lopez, F. Gonzales–Caballero, J.D.G. Duran, Rheological study of the stabilization of magnetizable colloidal suspensions by addition of silica nanoparticles, *J. Rheol.* 47 (2003) 1093–1109.

FIGURES AND TABLES CAPTIONS

Fig. 1. XPS spectra for CI samples without and with exposure to Ar + C₄F₈ plasma.

Fig. 2. Atomic ratio of F/Fe for CI samples without and with exposure to Ar + C₄F₈ plasma.

Fig. 3. Rheogram of 80 wt.% MR fluids based on samples A (open triangles) and B (lines) under various magnetic fields applied.

Fig. 4. Storage, G' , (solid symbols or line) and loss, G'' , (open symbols or dashed line) moduli versus strain, γ , at angular frequency of 62.83 rad s^{-1} for 80 wt.% MR fluid based on samples A (lines) particles under magnetic flux density (T) of 0 or 0.3, and B (symbols) particles under various magnetic fields applied. The symbols for magnetic flux densities (T): (●,○) 0; (▼,▽) 0.1; (■,□) 0.2; (▲,△) 0.3.

Fig. 5. Storage, G' , (solid symbols or line) and loss, G'' , (open symbols or dashed line) moduli versus angular frequency, ω , for samples A (lines) particles under magnetic flux density (T) of 0 or 0.3, and B particles based MR suspension (80 wt.%) under various magnetic fields applied. The symbols for magnetic flux densities (T): (●,○) 0; (▼,▽) 0.1; (■,□) 0.2; (▲,△) 0.3.

Fig. 6. Sedimentation ratio versus time for sample A (■), B (▲), C (▼) based MR suspensions (50 wt.%) in 200 mPa s silicone oil.

Table 1. Parameters of samples and their surface composition from XPS.

Table 2. Parameters of the Cho–Choi–Jhon model obtained by linear regression for various treated CI particles–based MR fluids at the magnetic flux density of 0.3 T.